Available online at www.sciencedirect.com
SCIENCE DIRECT®
Solid State Communications 128 (2003) 419–423
solid state communications
www.elsevier.com/locate/ssc

Characterization of Na precipitates in electron irradiated NaCl crystals by wide angle X-ray scattering (WAXS)

S.N. Sulyanov[a], D.M. Kheiker[a], D.I. Vainshtein[b], H.W. den Hartog[b,*]

[a]*Institute of Crystallography, RAS, 119333, Leninsky pr. 59, Moscow, Russian Federation*
[b]*University of Groningen, Nijenborgh 4, NL-9747 AG Groningen, The Netherlands*

Received 13 February 2003; received in revised form 31 July 2003; accepted 4 September 2003 by T.T.M. Palstra

Abstract

Samples of synthetic NaCl crystals have been exposed to different doses of electron irradiation up to 1500 MGy (150 Grad) at elevated temperatures, and studied subsequently by X-ray diffraction. Our experimental results clearly show that there is a close correspondence between the geometrical properties (such as lattice distances and the crystal orientation) of the host crystal and the radiation-induced Na precipitates, which is referred to as the Kurdjumov–Sachs orientation relationship (K–S OR). The size of the precipitates has been estimated.

PACS: 61.10.Eq; 61.10.Nz; 61.46. + w; 61.72. − y; 61.80.Fe; 81.30.Mh

Keywords: A. NaCl; A. Precipitate; C. X-ray scattering; D. Radiation effects; D. Orientation relationship

1. Introduction

Information from a variety of independent experiments (e.g. calorimetry, electron paramagnetic resonance (EPR), AC conductivity, nuclear magnetic resonance (NMR), optical absorption spectroscopy, Raman scattering, and atomic force microscopy) has shown that during exposure of NaCl (*fcc*) to ionizing radiation at elevated temperatures (e.g. 100 °C) with increasing dose increasing amounts of metallic Na (*bcc*) and chlorine bubbles are formed [1–10]. Until now the physical properties of the metallic Na precipitates have been studied most extensively, and these investigations have shown that quite often the Na nanoparticles behave anomalously.

The aim of the present work was to investigate the nature of the Na precipitates and characterize them independently by means of wide angle X-ray diffraction methods.

2. Experimental

2.1. Sample preparation, irradiation and characterization

The NaCl samples used for this investigation have been prepared in a pure He-atmosphere in carbon crucibles, by means of a modified Bridgman technique using a high frequency furnace. The impurities (KCl or KBF_4) were added to the raw NaCl material prior to crystal growth. The diameter of the cylindrical single crystals was 6 mm and thin disk shaped samples with a thickness of 0.5 mm were cut from the boules and polished afterwards. As many as 300 of these samples can be accommodated in the sample holder with a surface area of about 300 cm^2, which is irradiated in vacuum by 0.5 MeV electrons from a linear accelerator. The samples were irradiated at temperatures between 50 and 150 °C, and doses up to 1500 MGy (150 Grad) have been used for the present investigations.

To characterize the samples we have carried out latent heat measurements with our Perkin Elmer DSC-7 calorimeter setup. The latent heat of melting of the metallic Na-precipitates provides information about the amount of radiolytic Na in the sample [3]. We note that the melting

* Corresponding author. Fax: +31-50-363-4879.
E-mail address: h.w.den.hartog@phys.rug.nl (H.W. den Hartog).

0038-1098/$ - see front matter © 2003 Elsevier Ltd. All rights reserved.
doi:10.1016/j.ssc.2003.09.006

temperature of bulk Na is about 97 °C, whereas the latent heat peak of melting of radiolytic Na in NaCl is often at a different position, probably due to size effects [3].

2.2. The single crystal experiments

We have used a Bruker Apex diffractometer with a 2D-CCD (512 × 512) detector to carry out single crystal experiments. The investigated samples were cleaved and had an oblong shape, and a diameter of about 0.3 mm. During the experiment they were glued by one end on the holder, such that the incident beam did not touch the cement during the exposure to minimize the background scattering. The samples were mounted approximately along the φ-axis of the goniometer, which has a standard inclination angle of 54.72°. Mo K_α-radiation and a graphite monochromator were used. The X-ray generator voltage was reduced to 34 kV to avoid $\lambda/2$ contributions from white spectrum. One hundred and eighty successive patterns with φ-step of 1° were registered. During each exposure the sample was rotated within $\Delta\varphi = \pm 0.5°$ to average the intensity. To achieve the required high ratio of pixel intensities, several measurements as described above for each φ-angle have been carried out and averaged later on (using this procedure the dynamic range of the observations, I_{max}/I_{min}, has been improved to a value of about 10^5). This methodology was crucial for this task (the observation of both the very weak spots from Na precipitates and strong peaks from the NaCl matrix). The laboratory coordinates were chosen so that the Z-axis was along the φ-rotation axis.

In general, the orientation matrix (OM) is used to describe a rotation of a solid body relative to the laboratory coordinate system. If $\hat{\mathbf{A}}$ is the OM for a crystal (i.e. the NaCl crystal or the Na-precipitate in our case, we consider further only cubic crystals for simplicity), then any unit vector can be written in both the laboratory ($\mathbf{r}$) and crystallographic unit basis ($\mathbf{n}$) using the relation: $\mathbf{r} = \hat{\mathbf{A}}\mathbf{n}$. In accordance with this relation we can write $\mathbf{n}_{NaCl} = \hat{\mathbf{A}}^{-1}_{NaCl}\mathbf{r}_{NaCl}$.

Actually, any OM can be chosen from a set of equivalent matrices. Each one from this set can be obtained by multiplication OM by a matrix $\hat{\mathbf{W}}_i$ representing one of the point group rotation operators for the crystal under investigation. Any vector $\mathbf{n}_{Na}$ corresponding to a reflection from Na precipitate, can be written in 'NaCl' coordinates as $\mathbf{n}_{Na} = \hat{\mathbf{W}}_i\hat{\mathbf{U}}\mathbf{n}_{NaCl}$ ($i = 1, N_w$). Here $N_w = 24$ for the point group $m\bar{3}m$ and $\hat{\mathbf{U}}$ is any matrix connecting NaCl and Na systems. Obviously, if p is the multiplicity factor for a particular crystallographic coordinate plane of the precipitate, and N_w is the number of $\hat{\mathbf{W}}$-matrices for the host crystal, then the total number of possible reflections in the diffraction pattern can be $P = pN_w$. So if we use hkl-type reflections for the Na precipitates, then in general as many as $48 \times 24 = 1152$ reflections are possible. We chose the 200-type reflections ($p = 6$) from the Na precipitates to determine their orientations. First of all we consider here sample 1 with a maximum irradiation dose and the highest concentration of Na-precipitates (see Table 1). It is well known, that the OM elements a_{ij} can be written in terms of trigonometric functions with three Eulerian angles. We have used this representation of $\hat{\mathbf{A}}_{NaCl}$ to calculate these angles for the NaCl crystal by means of a least-squares fitting method. After the $\hat{\mathbf{A}}^{-1}_{NaCl}$ transformation we considered all vectors corresponding to the observed 200-type Na reflections in the coordinate system of NaCl (Fig. 1). Initially we chose only three mutually perpendicular vectors to calculate the $\hat{\mathbf{U}}$-matrix and to preliminarily generate all possible vectors using $\hat{\mathbf{W}}_i$-matrices and adding to this set the inverted vectors as well. It turned out that all 83 vectors measured by 200-type reflections belonged to the same orientation. Then we calculated the $\hat{\mathbf{U}}$-matrix by direction cosines of these 83 vectors applying the proper $\hat{\mathbf{W}}_i$-matrices to ascribe them to only 200-type indices. Mean absolute angular deviation between the calculated and measured directions was 0.81°.

It is worth to note that we did not find any evidence for the presence of polycrystalline metallic Na by means of single crystal X-ray diffraction.

2.3. The powder experiments

The geometry used in the Bruker diffractometer did not allow us to achieve an angular resolution better than about

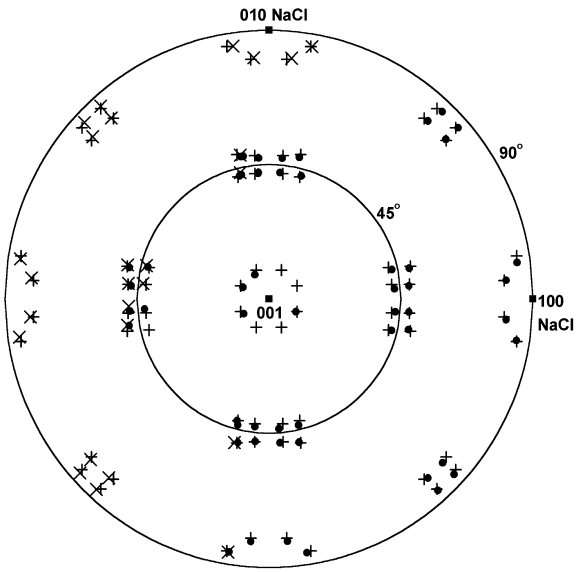

Fig. 1. Projection of the ⟨001⟩ directions of Na precipitates in the unit cell coordinate system of NaCl crystal. '●'—the measured vector is in the upper half-sphere, 'x'—in the bottom half-sphere (inverted vector is shown). ' + '—all vectors are generated for K–S OR.

Table 1
Samples studied

% Na (DSC)	Dose (Grad)	Dose rate (Mrad/h)	Irradiation temperature (°C)	a_{NaCl} (Å)	a_{Na} (Å)	Estimated precipitate size (Å)	Number of observed *bcc* Na lines	V_{Na}/V (%)
9.33	150	100	100	5.635(4)	4.279(4)	340	5	7.8
2.86	150	250	100	5.634(4)	4.269(7)	130	2	4.2
2.81	105	100	110	5.635(4)	4.289(4)	340	4	2.3
1.00	150	250	60	5.633(4)	Not measured	Not determined	1	–
Un-irradiated NaCl	–	–	–	5.634(4)	–	–	–	–

0.7°. This resolution is not sufficient to estimate the line broadening and the associated size of the Na precipitates.

To determine the line broadening and Na volume percentage in a more straightforward way than in single crystal experiments we have used the KARD6 diffractometer with a 256×256 2D-detector [11]. Cu K_α-radiation and a graphite monochromator were used. The angular resolution of this experiment was $\Delta(2\theta) = 0.18°$ (full width at half-maximum (FWHM) of the instrumental resolution function (IRF), θ is the Bragg angle). The single crystal samples were crushed in a mortar down to about 40 μm grain size (this quite large size was used to avoid serious interaction between Na precipitates in the NaCl host crystal and the surrounding atmosphere). After this the coarse grain powder was inserted into a glass capillary with a diameter of 0.7 mm. The capillary was rotated about the vertical θ-axis during the exposure. Several reloads were used to improve the averaging over the individual grains. The procedure described in [11] was applied to calculate the intensity vs. the scattering angle function $I(2\theta)$, i.e. a powder pattern of sufficient quality was obtained by averaging the intensity over the whole detector plane. Then we calculated the FWHM for the strongest Na 110 line by profile fitting and compared it with the well-known FWHM of the IRF, which in this case is very close to Gaussian [11]. The powder patterns for two samples are presented in Fig. 2. The small intensity of the Na peak is the reason for the reduced accuracy of its shape determination, and so the precise determination of the broadening function by deconvolution with the IRF was difficult. We have used a simple Gaussian–Gaussian approximation as an estimate. The average size of Na precipitates was obtained from the Scherrer formula $L = 0.89\lambda/(\cos\theta\Delta(2\theta))$. Here, $\Delta(2\theta) = (B^2 - b^2)^{1/2}$, B and b are measured and reference FWHM values; λ is the wavelength of the X-rays. The results are summarized in Table 1.

To estimate the volume fraction of the Na precipitates in the sample we have assumed that the Na and NaCl polycrystalline phases contribute to the Bragg line intensity independently, and the combined temperature factor is the same for both phases.

As is known, the Bragg line intensity for a powder pattern (without taking into account the absorption factor) is proportional to the expression

$$I \sim (1/\Omega^2)pF_{hkl}^2(1 + \cos^2 2\theta)/(\sin^2\theta\cos\theta)V = kV,$$

where Ω is a unit cell volume, p is the multiplicity factor, F_{hkl} is a structure amplitude for indices hkl, and V is the powder volume.

So, if $I_{NaCl} = k_{NaCl}V_{NaCl}$, and $I_{Na} = k_{Na}V_{Na}$, then

$$(V_{Na}/V_{NaCl}) = (k_{NaCl}/k_{Na})(I_{Na}/I_{NaC});$$

and, finally the volume percentage of Na in the sample is $x_V = 1/(1 + V_{NaCl}/V_{Na})$.

The data are summarized in Table 1.

3. Results and discussion

As is known, *fcc* and *bcc* lattices can have different orientation relationships. In particular they are considered in the theory of martensite transformations (see for example [12]), epitaxy [13], and metal–metal precipitation [14,15]). K–S OR [16] is generally designated by two conditions:

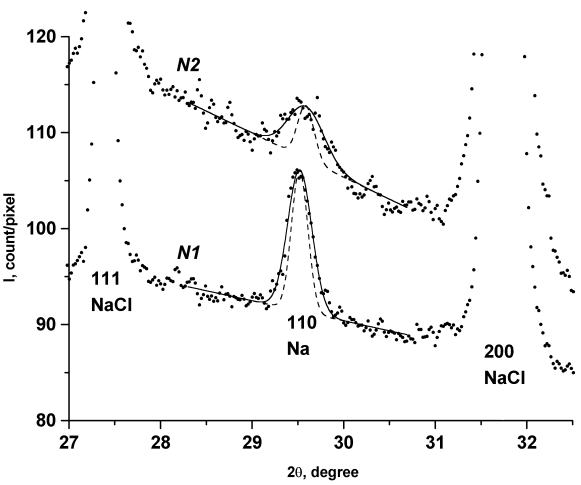

Fig. 2. X-ray powder patterns measured, Gaussian $K_{\alpha 1,2}$-doublet peak fitting (solid line) and Gaussian IRF (dashed line) for samples 1,2.

$(1\ -\ 11)_f \| (101)_b$ and $[101]_f \| [1\ -\ 11]_b$. Note that the rotation matrix defined by these indices does not correspond to the smallest rotation angle. Among all equivalent matrices the one with the smallest rotation angle δ from the set $\delta_i = a\cos([\mathrm{Tr}(\hat{\mathbf{S}}_i) - 1]/2)$, where $\hat{\mathbf{S}}_i$ are equivalent matrices describing K–S OR, should be chosen for simplicity and definiteness. The smallest value of $\delta = 42.85°$ corresponds (for example) to the conditions $(-1\ -\ 11)_f \| (0\ -\ 11)_b$ and $[101]_f \| [111]_b$. The rotation axis in this case is defined by the direction cosines $c_1 = -0.178$, $c_2 = 0.178$, $c_3 = 0.968$, i.e. it is inclined by 14.55° from the [001] axis of the *fcc* (NaCl) host crystal (here $c_1 = (s_{32} - s_{23})/2\sin\delta$, $c_2 = (s_{13} - s_{31})/2\sin\delta$, $c_3 = (s_{21} - s_{12})/2\sin\delta$, s_{kl} are the transformation matrix elements). The $\hat{\mathbf{W}}\hat{\mathbf{U}}$-matrix and the $\hat{\mathbf{S}}$-matrix are very close. The transformation $\hat{\mathbf{S}}(\hat{\mathbf{W}}\hat{\mathbf{U}})^{-1}$ corresponds to a residual rotation angle of 0.31°. This implies that the Na precipitates in NaCl have K–S OR within the accuracy of our measurements. This OR was found for all investigated samples where at least the 110-type Na reflections were registered. The accuracy of the calculation was reduced for samples with low Na contents. The numbers of possible *bcc* reflections were different for the samples with different Na contents. We have found five first line spots by means of the single crystal method for sample 1 and only weak spots of the 110-type for sample 4. It suggests that the lattice of the precipitates is distorted.

It is beyond the scope of this paper to dwell at length on the theories of epitaxy [13]. Our precipitate system is more complex than those encountered in the literature on epitaxial growth, because (i) in contrast with epitaxial growth of a metal on the surface of another metal, the interface NaCl:Na is 3D, and (ii) the host crystal (with ionic bonding) consists of two sub-lattices with different charges, while in the precipitate we are dealing with metallic bonds. Nevertheless if we assume that the Na layer in {111} NaCl plane can be considered as a metal mono-layer on the plane {110} of the single-crystalline Na, then the epitaxy model can be used.

So, with the assumption above we will give just a brief explanation of our results below by considering the Na-precipitate lattice and the Na-sublattice of the NaCl crystal on the basis of the theory of epitaxy.

According to the model calculation (see Ref. [13]), in cases where the ratio has the special value $r = a/b = 1.0887$ (with a equal to the nearest neighbor distance in a plane {111} of the *fcc* crystal and with b equal to the corresponding value in the {110} plane of the *bcc* crystal), one can achieve a good match along the closest packed row of these lattices by rotating one layer through the angle $\Theta = 5.26°$. This situation corresponds to K–S OR. In cases where $r = 0.95$ and $\Theta = 0°$, the Nishiyama–Wasserman (N–W) OR occurs, i.e. $\{111\}_f \| \{110\}_b$ and $\langle 110\rangle_f \| \langle 100\rangle_b$. Also it is important to note that the total energy of the epitaxial system *fcc*/*bcc* $\{111\} \| \{110\}$ is a function of r and Θ. When $\Theta = 5.26°$ the curve shows its deepest minimum for the r value, which corresponds with K–S OR and when $\Theta = 0°$ the minimum is found for the r value, which corresponds with N–W OR, respectively. The energy turns out to be independent of r for all other values of Θ.

The nearest neighbor distance of the Na sub-lattice for the Na {111} plane in the NaCl crystal is $a = 3.984$ Å and the corresponding distance in the Na precipitate is $b = 3.706$ Å. This implies that the ratio is $r = 1.075$, which is quite close to the value for K–S OR mentioned above. As it has been noted, unstrained K–S OR or N–W OR behavior does not exist. A vast richness of structures opens up when the slightest atomic relaxations are allowed to take place. The structural phase diagram of bi-crystals as a function of the geometrical and energetic parameters has been considered [13].

Note, that as it has been revealed in Ref. [17], the system Li–LiH with $r = 0.947$, represents the almost ideal situation for the occurrence of N–W OR.

4. Concluding remarks

(1) Nanoparticles of metallic Na with sizes of about 100–300 Å depending on the conditions and dose of electron irradiation, are present in the NaCl matrix. (2) Within the experimental error all Na nanoparticles have Kurdjumov–Sachs orientation relative to the NaCl matrix. (3) Polycrystalline metallic Na has not been detected by means of single crystal X-ray diffraction methods.

Acknowledgements

The work was partly financed by NWO (grant number 047.008.021) and RFFI (grant number 00-15-9633).

References

[1] J.C. Groote, J.R.W. Weerkamp, J. Seinen, H.W. den Hartog, Phys. Rev. B 50 (1994) 9798.
[2] J. Seinen, J.C. Groote, J.R.W. Weerkamp, H.W. den Hartog, Phys. Rev. B 50 (1994) 9793.
[3] J.R.W. Weerkamp, J.C. Groote, J. Seinen, H.W. den Hartog, Phys. Rev. B 50 (1994) 9781.
[4] D.I. Vainshtein, H.P. den Hartog, H.C. Datema, J. Seinen, H.W. den Hartog, Radiat. Eff. Defects Solids 137 (1995) 73.
[5] D.I. Vainshtein, H.W. den Hartog, Appl. Radiat. Isot. 47 (1996) 1503.
[6] H.W. den Hartog, J.C. Groote, J.R.W. Weerkamp, Radiat. Eff. Defects Solids 139 (1996) 1.
[7] O. Kanert, C. Schmidt, R. Küchler, H.W. den Hartog, Ber. Bunsen-Ges. 101 (9) (1997) 1286.
[8] H.W. den Hartog, Radiat. Eff. Defects Solids 150 (1999) 167.

[9] D.I. Vainshtein, H.W. den Hartog, Radiat. Eff. Defects Solids 152 (2000) 23.
[10] E.I. Shtyrkov, A. Klimovitskii, H.W. den Hartog, D.I. Vainshtein, J. Phys.: Condens. Matter 14 (2002) 9053.
[11] S.N. Sulyanov, A.N. Popov, D.M. Kheiker, J. Appl. Cryst. 27 (1994) 934.
[12] R.W. Cahn, P. Haasen (Eds.), Physical Metallurgy, North-Holland Physics Publishing, Amsterdam, 1996.
[13] A. Zangwill, Physics at Surfaces, Cambridge University Press, London, 1996.
[14] J.K. Chen, D. Farkas, W.T. Reynolds, Acta Mater. 40 (11) (1997) 4415.
[15] S.P. Luo, U. Dahmen, Acta Mater. 46 (6) (1998) 2063.
[16] G.V. Kurdjumov, G. Sachs, Z. Phys. 64 (1930) 325.
[17] G.S. Smith, J. Phys. Chem. Solids 36 (1975) 797.